MicroRNA-126 and VEGF enhance the function of endothelial progenitor cells in acute myocardial infarction

YING ZHANG, YI XU, KE ZHOU, GUOYING KAO and JUN XIAO

Department of Cardiovascular Medicine, Chongqing Emergency Medical Center
(Fourth People's Hospital of Chongqing), Chongqing 400014, P.R. China

Abstract. Previous studies have found that microRNA-126 (miR-126) overexpression can exert beneficial effects on endothelial function and angiogenesis. The role of miR-126 was previously reported to be by directly limiting the activities of negative regulators of the vascular endothelial growth factor (VEGF) pathway, such as PI3K regulation subunit 2 (PIK3R2). The aim of the present study was to investigate the role of the miR-126/PIK3R2/VEGF axis in endothelial progenitor cells (EPCs) under hypoxic conditions. An *in vitro* hypoxia model in EPCs was established by exposing EPCs to hypoxia ($O_2/N_2/CO_2$, 1/94/5) for 72 h, before reverse transcription-quantitative PCR (RT-qPCR) and western blot analyzes were used to measure miR-126 and PIK3R2 expression in EPCs. The proliferation, migration and tube-forming ability of the transfected cells were measured using MTT, Transwell and tube formation assays, respectively. miR-126 expression was found to be lower in EPCs in the hypoxia group compared with that in the control group (P<0.01). The expression of PIK3R2, a direct target gene of miR-126, was found to be higher in the hypoxia group compared with that in the control group (P<0.01). miR-126 mimic and VEGF-plasmid co-transfection improved the proliferation, migration, tube-forming ability and restored the phosphorylation of AKT in EPCs under hypoxic conditions (all P<0.01). In addition, the effects of miR-126 mimic on hypoxia-induced EPCs were reversed by PIK3R2-plasmid co-transfection, whilst the effects of VEGF-plasmid were enhanced further by co-transfection with the miR-126 mimic. In conclusion, miR-126 promoted the functions of EPCs under hypoxic conditions by negatively targeting PIK3R2, whilst the combined overexpression of miR-126 and VEGF enhanced these aforementioned effects.

Correspondence to: Dr Jun Xiao, Department of Cardiovascular Medicine, Chongqing Emergency Medical Center (Fourth People's Hospital of Chongqing), 1 Jiankang Road, Yuzhong, Chongqing 400014, P.R. China
E-mail: xiaojun091112@163.com

Introduction

Ischemic heart disease, particularly acute myocardial infarction (AMI), causes 2-4 million deaths in the USA, >4 million deaths in Europe and northern Asia (1) and is responsible for >33% deaths in developed nations annually (2). AMI is a severe heart condition that is caused by sudden interruptions of the blood circulation in part of the cardiac muscle, which in turn results in the lack of sufficient oxygen to this key organ (3-5). The main pathological processes of MI include ischemia and hypoxia (6). MI is characterized by severe and persistent thoracic pain, fever, increased white blood cell count, increased red blood cell sedimentation rate, increased serum cardiac enzyme (creatine kinase MB and cardiac troponin I) levels and electrocardiographic changes (such as ST segment elevation), which may lead to arrhythmia, shock or heart failure (7-9). Therefore, effective restoration of blood flow is crucial (10). Previous studies have reported that several types of stem cells, particularly endothelial progenitor cells (EPCs), can improve new blood vessel formation in local ischemic areas safely and effectively (11,12). EPCs has been used for AMI investigation *in vitro* (13-15). For these reasons, EPCs were used in the present study.

MicroRNAs (miRNAs/miRs) are a class of small RNAs that are 20-22 nucleotides in length and regulate post-transcriptional gene expression in plants and animals (16,17). miRNAs serve a variety of important regulatory functions (18). Each miRNA may have multiple target genes, whereas several different miRNAs can regulate the same gene (19). This complex regulatory network can regulate the expression of multiple genes through a single miRNA or a combination of several miRNAs to fine-tune the expression profile (19). Previous studies have suggested roles for miRNAs in numerous human diseases, including cardiovascular, gynecological, neurological and urinary system diseases, as well as cancer (20-22). An increasing number of studies have found that miRNAs serve an important role in processes of blood vessel formation and repair, which are crucial for angiogenesis (23,24). Recently, miR-126, which participates in endothelial cell function and angiogenesis, was reported to be highly expressed in EPCs (25). Previous studies have found that miR-126 acts by directly regulating the expression of negative regulatory factors of the VEGF pathway, such as Spred-1 protein and PI3K regulation sub-base 2 (PIK3R2) (26-28). Therefore, upregulating the expression of Spred-1 or suppressing the expression of VEGF may mediate similar effects to miR-126 knockout (26,29). In addition,

another study previously reported that miR-126 can negatively regulate VEGF expression in hypoxia-induced monkey chorio-retinal vessel endothelial cells (30). However, whether miR-126 can regulate angiogenesis and/or VEGF expression in AMI has not been elucidated.

Therefore, the present study aimed to investigate the effects of the miR-126/PIK3R2/VEGF axis in EPCs under hypoxic conditions. In addition, the present study explored the possible underlying molecular mechanism to provide a theoretical basis for the development of novel clinical strategies for the treatment of AMI.

Materials and methods

Cell culture and establishment of a hypoxia EPC model. EPCs from human peripheral blood (cat. no. CC-H163; Shanghai Enzyme Research Biotechnology Co., Ltd.; http://www.elisakits.cn/Index/productInfo/cid/148/id/769.html) were cultured in endothelial cell growth medium-2 (Gibco; Thermo Fisher Scientific, Inc.) supplemented with 10% FBS (Gibco; Thermo Fisher Scientific, Inc.) and incubated at 37°C with 5% CO_2. EPCs were exposed to hypoxia ($O_2/N_2/CO_2$, 1/94/5%) at 37°C for 72 h to establish the cell model of hypoxic injury. EPCs cultured under normoxic conditions served as the control. The study was approved by the Ethics Committee of Chongqing Emergency Medical Center (Fourth People's Hospital of Chongqing; Chongqing, China).

Luciferase reporter analysis. Previous studies have reported the binding sites between PIK3R2 and miR-126 (27,28). To verify the binding sites between miR-126 and PIK3R2, dual-luciferase reporter assay was performed. Briefly, the 3'-untranslated region (UTR) of PIK3R2, which contained the miR-126 binding site or a mutated target site, was synthesized by reverse transcription (RT) PCR using a PrimeScript™ RT reagent kit (cat. no. RR037A; Takara Bio, Inc.). The temperature protocol was 5 min at 25°C followed by 60 min at 42°C. The wild type (WT-PIK3R2) and mutant (MUT-PIK3R2) 3'-untranslated regions (UTR) of PIK3R2 were cloned into the pmiR-RB-Report™ dual-luciferase reporter gene plasmid (Guangzhou RiboBio Co., Ltd.) following the manufacturer's protocols. 293T cells [ATCC; cultured in DMEM (Gibco; Thermo Fisher Scientific, Inc.) supplemented with 10% FBS at 37°C with 5% CO_2] were co-transfected with 1 µg WT-PIK3R2 or 1 µg MUT-PIK3R2 and 50 nM miR-126 mimic (5'-UCGUACCGUGAGUAAUAAUGCG-3'; Guangzhou RiboBio Co., Ltd.) or 50 nM mimic control (5'-UAGUCAACG AGUCUAUGAGUCG-3'; Guangzhou RiboBio Co., Ltd.) using Lipofectamine® 2000 (Invitrogen; Thermo Fisher Scientific, Inc.). In total, 48 h after transfection, the relative luciferase activity was assessed using the Dual-luciferase reporter assay system (Promega Corporation) and normalized to *Renilla* luciferase, according to the manufacturer's protocols.

RNA extraction and reverse transcription-quantitative (RT-q) PCR analysis. Total cellular RNA was obtained using TRIzol® reagent (Invitrogen; Thermo Fisher Scientific, Inc.) and then the RNA was reverse-transcribed to cDNA via a RevertAid First Strand cDNA Synthesis Kit (cat. no. K1621; Invitrogen; Thermo Fisher Scientific, Inc.). The reaction conditions were as follows: 70°C for 5 min, 37°C for 5 min and 42°C for 60 min.

In accordance with the manufacturer's protocol, all reactions were performed using the ABI Prism 7000 Real Time PCR system with SYBR Green ER™ qPCR SuperMix Universal (cat. no. 11762100; Invitrogen; Thermo Fisher Scientific, Inc.) to quantify the relative gene expression. The themocycling conditions consisted of the following steps: 5 min at 95°C, followed by 40 cycles at 95°C for 10 sec and 60°C for 30 sec. U6 or GAPDH was used as the internal control. Primers were supplied by Sangon Biotech Co., Ltd and listed as following: miR-126 forward, 5'-TATGGTTGTTCTCGACTCCTTCAC-3' and reverse, 5'-TCGTCTGTCGTACCGTGAGTAAT-3'; U6 forward, 5'-CTCGCTTCGGCAGCACA-3' and reverse, 5'-AAC GCTTCACGAATTTGCGT-3'; PIK3R2 forward, 5'-GCA CCACGAGGAACGCACTT-3' and reverse, 5'-CGTCCACTA CCACGGAGCAG-3'; AKT forward, 5'-TAAAGAAGGAGG TCATCGTGG-3' and reverse, 5'-CGGGACAGGTGGAAGA AAA-3' and GAPDH forward, 5'-CTTTGGTATCGTGGA AGGACTC-3' and reverse, 5'-GTAGAGGCAGGGATGATGT TCT-3'. The related mRNA expression levels of miR-126, PIK3R2 and AKT were calculated by using the $2^{-\Delta\Delta Cq}$ method (31).

Western blot analysis. EPCs were lysed using RIPA buffer (Beyotime Institute of Biotechnology). The cell lysates were centrifuged at 10,000 x g at 4°C for 15 min to obtain total protein. Subsequently, the protein was quantified by using a bicincho-ninic acid protein kit (Beyotime Institute of Biotechnology) and equal amount of proteins (40 µg per lane) was separated by 10% SDS-PAGE, followed by transfer to PVDF membranes. The membranes were then blocked at room temperature for 1 h in PBST (0.1 % Tween-20) solution containing 5% non-fat milk. Subsequently, the membranes were incubated with PIK3R2 (cat. no. ab180967; dilution: 1:2,000; Abcam), phosphorylated (p-)-AKT (cat. no. 4060; dilution: 1:1,000; Cell Signaling Technology, Inc.), AKT (cat. no. 4685; dilution: 1:1,000; Cell Signaling Technology, Inc.) or GAPDH (cat. no. 5174; dilution: 1:1,000; Cell Signaling Technology, Inc.) primary antibodies at 4°C overnight. The membranes were then washed three times with PBST and incubated with the goat anti-rabbit IgG H&L (HRP) secondary antibody (cat. no. ab6721; dilution: 1:3,000; Abcam) for 1 h at room temperature. The protein bands were visualized by an electrochemiluminescence (ECL) luminescent substrate (Pierce; Thermo Fisher Scientific, Inc.) following the manufacturer's protocols. ImageJ version 2.0 software (National Institutes of Health) was used to quantify the band intensities.

Cell transfection. EPCs during the logarithmic growth phase were inoculated into 6-well plates overnight and were transiently transfected with 1 µg Control CRISPR Activation Plasmid (control-plasmid; cat. no. sc-437275; Santa Cruz Biotechnology, Inc.), 1 µg PI 3-kinase p85β CRISPR Activation Plasmids (PIK3R2-plasmid; cat. no. sc-401991-ACT; Santa Cruz Biotechnology, Inc.), 1 µg VEGF CRISPR Activation Plasmids (VEGF-plasmid; cat. no. sc-400019-ACT; Santa Cruz Biotechnology, Inc.), 50 nM mimic control or 50 nM miR-126 mimic using the Lipofectamine® 2000 reagent (Invitrogen; Thermo Fisher Scientific, Inc.) according to the manufacturer's protocols. Following 72 h of transfection under hypoxic conditions at 37°C, the cells were collected to detect the transfection efficiency by RT-qPCR analysis and following experiments were performed. Cells were divided into the following groups:

i) Control group, where cells were cultured for 72 h under hypoxic conditions at 37˚C; ii) control-plasmid group, where cells were transfected with the control-plasmid for 72 h under hypoxic conditions at 37˚C; iii) VEGF-plasmid group, where cells were transfected with the VEGF-plasmid for 72 h under hypoxic conditions at 37˚C; iv) mimic control group, where the cells were transfected with the mimic control for 72 h under hypoxic conditions at 37˚C; v) miR-126 mimic group, where cells were transfected with the miR-126 mimic for 72 h under hypoxic conditions at 37˚C; vi) miR-126 mimic + control-plasmid group, where cells were co-transfected with the miR-126 mimic and control-plasmid for 72 h under hypoxic conditions at 37˚C; and vii) miR-126 mimic + VEGF-plasmid group, where cells were co-transfected with miR-126 mimic and VEGF-plasmid for 72 h under hypoxic conditions at 37˚C.

MTT assay. MTT assay was performed to evaluate cell viability. The cells ($1x10^4$ cells/well) were seeded into 96-well plates after transfection for 72 h, followed by addition of 5 mg/ml MTT (Beyotime Institute of Biotechnology) to each well and culture at 37˚C for 4 h. Subsequently, 100 μl DMSO was added into each well to solubilize the formazan crystals after the culture medium was removed. The absorbance was recorded at 570 nm using a microplate reader (Bio-Rad Laboratories, Inc.).

Transwell migration assay. The migration ability of the EPCs was detected using Transwell assay. The cells ($2x10^4$) were transferred onto upper chambers (8-μm pore size; BD Biosciences) suspended in a serum-free endothelial cell growth medium-2 after transfection for 72 h. At the same time, endothelial cell growth medium-2 supplemented with 10% FBS was added into the lower chambers. Following 24 h at 37˚C, cells that did not migrate and persisted on the upper surface of the filter were removed, before cells that had migrated to the lower surface of the membrane were fixed with 4% paraformaldehyde at room temperature for 30 min, stained with 0.1% crystal violet solution at room temperature for 15 min and imaged using a light microscope at x200 magnification. A total of three independent experiments were conducted.

Tube formation assay. The tube-forming ability of the EPCs was quantified by using Cultrex® *In Vitro* Angiogenesis Assay Tube Formation Kit (cat. no. 3470-096-K; Trevigen, Inc.) according to the manufacturer's protocols. For Basement Membrane Extract (BME) coating, 50 μl BME solution (contained within the kit) per well was added into the 96-well plate and the plate was incubated at 37˚C for 60 min. In total, $3x10^4$ EPCs were seeded into each well containing gelled BME and incubated in Endothelial Growth Medium-2 (Gibco; Thermo Fisher Scientific, Inc.) supplemented with 10% FBS (Gibco; Thermo Fisher Scientific, Inc.) and 30 ng/ml FGF-2 (Trevigen, Inc.) at 37˚C for 6 h. The mean number of complete tubes (a tube was defined as a linear sequence of cells linking two nodes) formed by EPCs was counted in five random fields of view under inverted light microscope at x100 magnification (TS100; Nikon Corporation).

Statistical analysis. Data are presented as the mean ± standard deviation from three independent experiments. The statistical significance of the differences among groups were analyzed either using unpaired Student's t test or one-way ANOVA
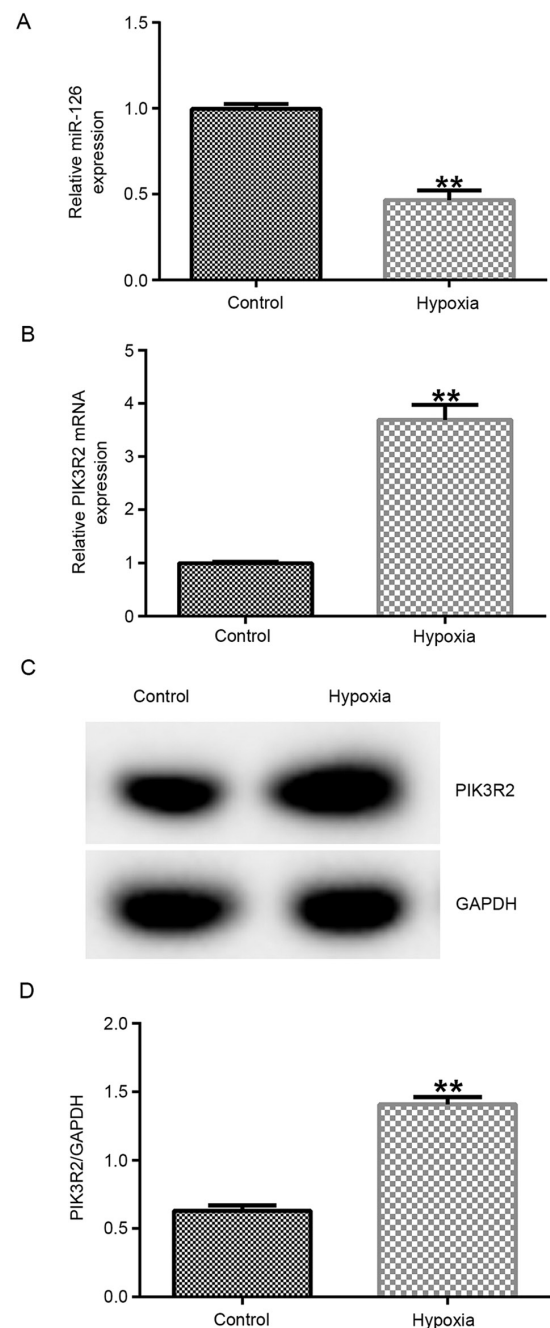

Figure 1. Expression of miR-126 and PIK3R2 in EPCs under hypoxic conditions. A hypoxia EPC model was established by exposing EPCs to hypoxia. RT-qPCR assay was performed to detect the mRNA expression levels of (A) miR-126 and (B) PIK3R2 in EPCs. (C) Western blot analysis was performed to measure the protein expression of PIK3R2 in EPCs, (D) which was quantified. **P<0.01 vs. Control. miR, microRNA; PIK3R2, PI3K regulation subunit 2; EPCs, endothelial progenitor cells.

followed by Tukey's post hoc test. P<0.05 was considered to indicate statistically significant differences.

Results

miR-126 expression is downregulated whereas PIK3R2 expression is upregulated in hypoxia-induced EPCs. The results demonstrated that the expression of miR-126 was significantly downregulated in the hypoxia group compared with that in the control group (Fig. 1A; P<0.01). Previous studies have shown
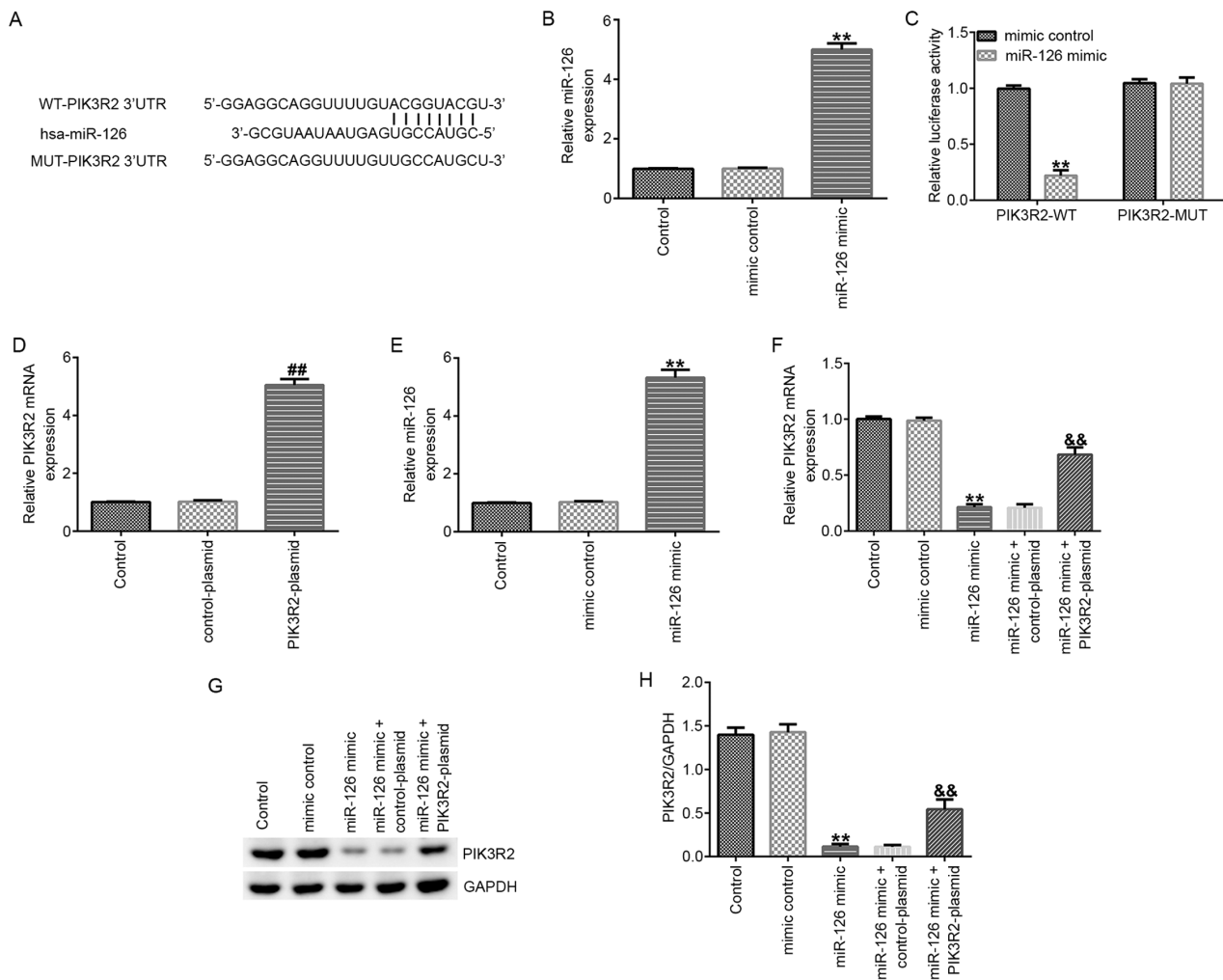
Figure 2. miR-126 overexpression negatively regulates PIK3R2 expression in EPCs. (A) Possible binding sites between miR-126 and PIK3R2 3'UTR. (B) 293T cells were transfected with the mimic control or miR-126 mimic for 48 h, before miR-126 expression was detected using RT-qPCR. (C) Potential interactions between miR-126 and PIK3R2 were assessed using dual-luciferase reporter assay. (D-H) EPCs were transfected with control-plasmid, PIK3R2-plasmid, mimic control, miR-126 mimic, miR-126 mimic + control-plasmid or miR-126 mimic+PIK3R2-plasmid under hypoxic conditions. (D) PIK3R2 and (E) miR-126 mRNA expression in EPCs was measured by RT-qPCR after plasmid or mimic transfection, respectively. (F) PIK3R2 mRNA expression in EPCs was measured by RT-qPCR after mimic and plasmid co-transfection. (G) PIK3R2 protein expression in EPCs was measured by western blot analysis, (H) which was quantified. **P<0.01 vs. mimic control. $^{\#\#}$P<0.01 vs. control-plasmid. $^{\&\&}$P<0.01 vs. miR-126 mimic + control-plasmid. miR, microRNA; UTR, untranslated region; WT, wild-type; MUT, mutant; RT-qPCR, reverse transcription-quantitative PCR; EPCs, endothelial progenitor cells; PIK3R2, PI3K regulation subunit 2.

that PIK3R2 is the target gene of miR-126 (27,28). Therefore, PIK3R2 expression was measured by RT-qPCR and western blot analyzes, which found it to be significantly increased at both mRNA (P<0.01) and protein levels in the hypoxia group compared with that in the control group (Fig. 1B-D).

miR-126 negatively regulates the expression of PIK3R2 in EPCs under hypoxic conditions. The possible binding sites between miR-126 and PIK3R2 were predicted (Fig. 2A) and verified using dual-luciferase reporter assay. Compared with that in cells transfected with the mimic control, miR-126 mimic transfection significantly enhanced miR-126 expression in 293T cells (Fig. 2B). Subsequently, compared with that in cells co-transfected with WT-PIK3R2 and mimic control, the luciferase activity of cells co-transfected with WT-PIK3R2 and miR-126 mimic significantly reduced (Fig. 2C). However, the luciferase activity of cells co-transfected with MUT-PIK3R2 and mimic control and cells co-transfected with MUT-PIK3R2

and miR-126 mimic exhibited no significant changes (Fig. 2C). Compared with that in their respective control plasmid and mimic groups, transfection with PIK3R2-plasmid or miR-126 mimic significantly increased the expression of PIK3R2 and miR-126 in EPCs under hypoxic conditions, respectively (Fig. 2D and E). In addition, miR-126 mimic transfection significantly reduced the expression of PIK3R2 at both mRNA and protein levels, whilst this reduction was significantly reversed by PIK3R2-plasmid co-transfection (Fig. 2F-H).

miR-126 affects the cell viability, migration and tube-forming ability of EPCs by targeting PIK3R2. Compared with those in the control group, the cell viability (Fig. 3A), tube-forming ability (Fig. 3B and C) and migration (Fig. 3D and E) of EPCs in the hypoxia group were significantly decreased. In addition, compared with those in the hypoxia + mimic control group, the proliferation (Fig. 3A), tube-forming ability (Fig. 3B and C) and migration (Fig. 3D and E) of EPCs in the
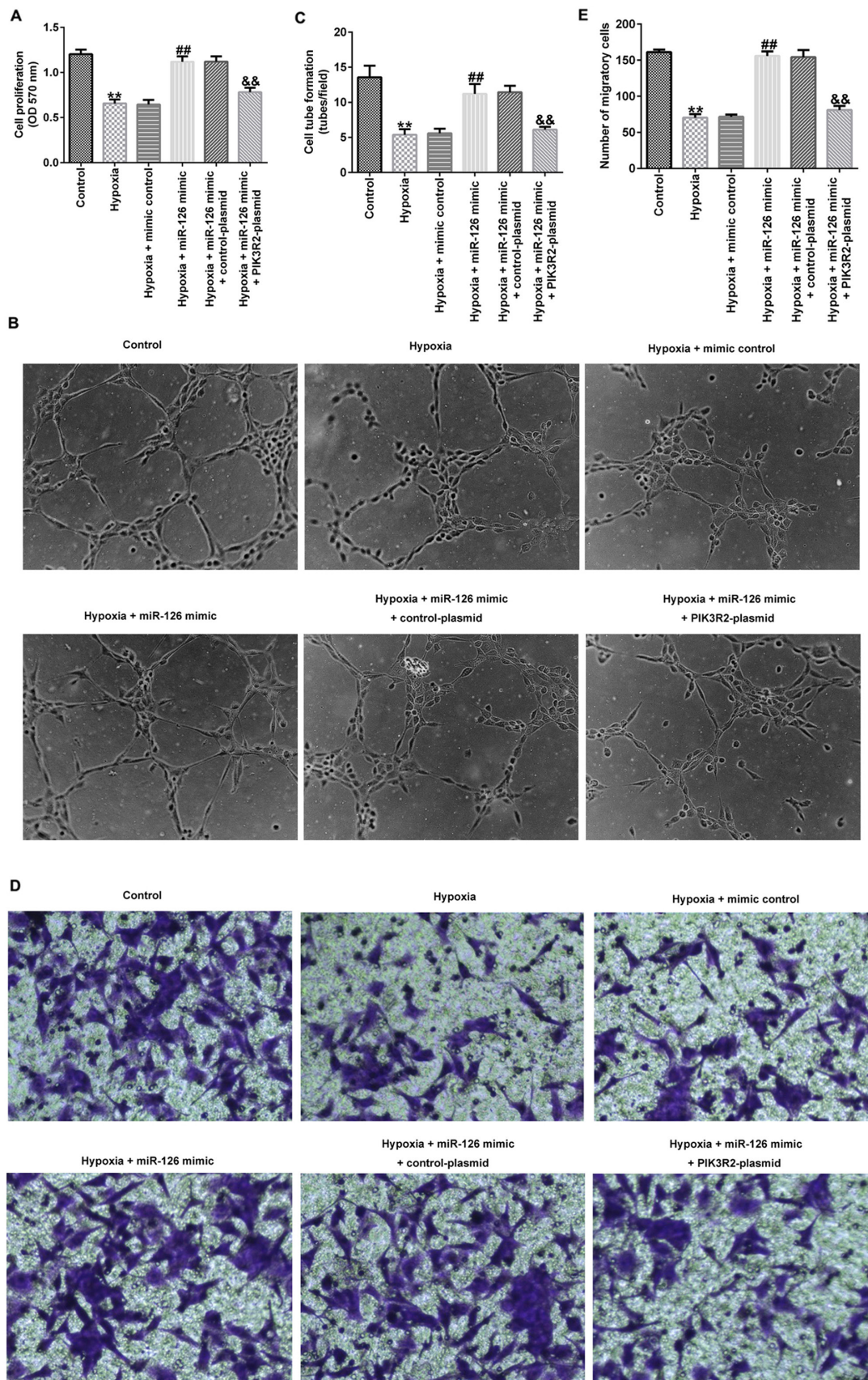
Figure 3. Effects of miR-126 mimic and PIK3R2-plasmid transfection on the viability, tube-forming ability and migration of EPCs under hypoxic conditions. EPCs were transfected with control-plasmid, PIK3R2-plasmid, mimic control, miR-126 mimic, miR-126 mimic + control-plasmid or miR-126 mimic + PIK3R2-plasmid under hypoxic conditions for 72 h. (A) MTT assay was performed to evaluate the cell viability of transfected EPCs. (B) Tube formation assay was used to measure the tube-forming ability of transfected EPCs. Magnification, x100. (C) Tube formation assay was quantified. (D) Transwell assay was used to measure the migration ability of transfected EPCs. Magnification, x200. (E) Transwell assay was quantified. **P<0.01 vs. Control. ##P<0.01 vs. hypoxia + mimic control. &&P<0.01 vs. hypoxia + miR-126 mimic + control-plasmid. miR, microRNA; PIK3R2, PI3K regulation subunit 2; OD, optical density; EPCs, endothelial progenitor cells.
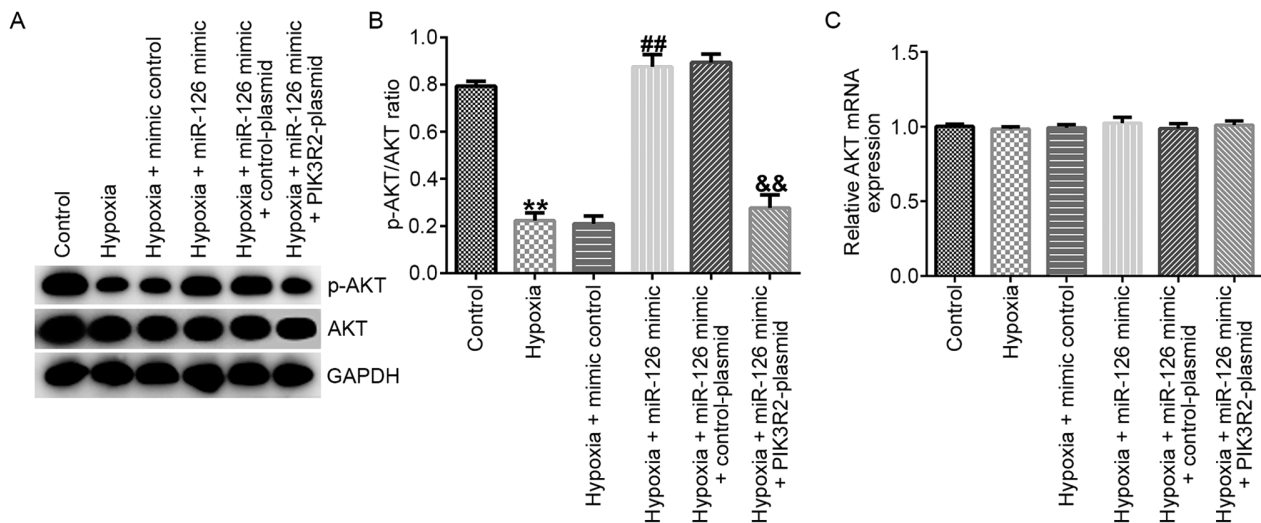
Figure 4. Effects of miR-126 mimic and PIK3R2-plasmid transfection on the PI3K/AKT pathway in EPCs under hypoxic conditions. EPCs were transfected with control-plasmid, PIK3R2-plasmid, mimic control, miR-126 mimic, miR-126 mimic + control-plasmid or miR-126 mimic + PIK3R2-plasmid under hypoxic conditions for 72 h. (A) Western blot analysis was used to measure the protein levels of p-AKT and AKT in transfected EPCs. (B) p-AKT/AKT ratio was quantified. (C) Reverse transcription-quantitative PCR was used to measure the mRNA expression levels of AKT in transfected EPCs. **P<0.01 vs. Control. $^{##}$P<0.01 vs. hypoxia + mimic control. $^{\&\&}$P<0.01 vs. hypoxia + miR-126 mimic + control-plasmid. miR, microRNA; p-, phosphorylated; EPCs, endothelial progenitor cells; PIK3R2, PI3K regulation subunit 2.
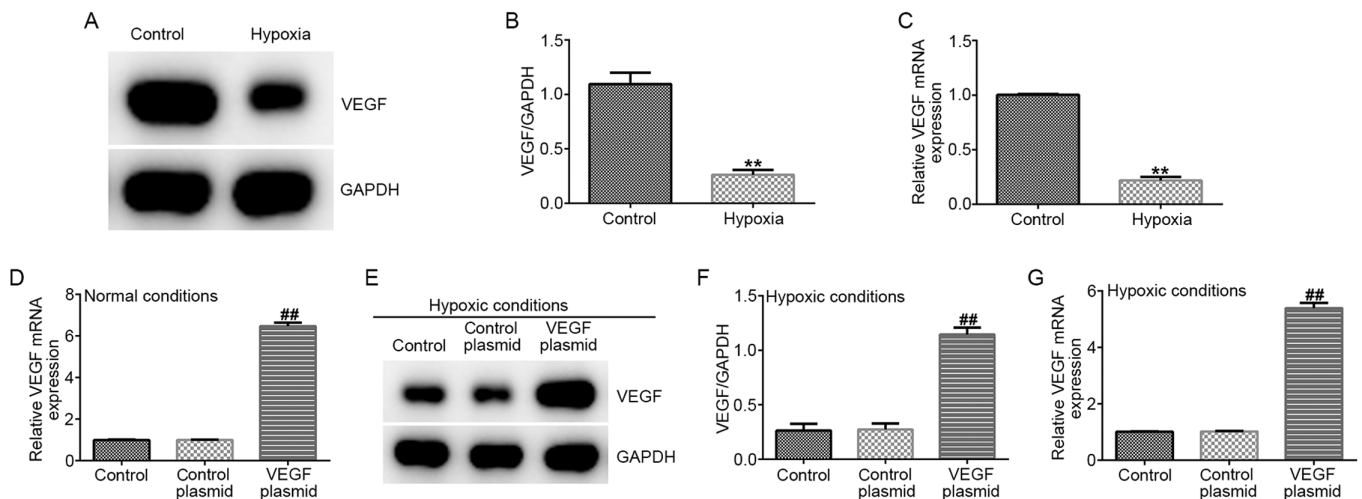

Figure 5. VEGF expression in EPCs under hypoxic conditions. A hypoxia EPC model was established through exposing cells to hypoxia. (A) Western blot assay was used measure the protein expression of VEGF in EPCs, (B) which was quantified. (C) RT-qPCR analysis was used to measure the protein and mRNA expression of VEGF in EPCs. (D) EPCs were transfected with control-plasmid or VEGF-plasmid under normal conditions for 72 h, then the mRNA expression of VEGF in EPCs was measured by RT-qPCR. (E-G) EPCs were transfected with control-plasmid, VEGF-plasmid under hypoxic conditions for 72 h. (E) Protein expression of VEGF in EPCs was measured by western blotting, (F) which was quantified (G) mRNA expression of VEGF in EPCs was measured by RT-qPCR analysis. **P<0.01 vs. Control. $^{##}$P<0.01 vs. control-plasmid. EPCs, endothelial progenitor cells; RT-qPCR, reverse transcription-quantitative PCR.

hypoxia + miR-126 mimic group were significantly increased, which were all significantly reversed by co-transfection with the PIK3R2-plasmid (Fig. 3A-E).

Western blotting and RT-qPCR assays were performed to measure the related protein and mRNA expression of AKT in EPCs. The results demonstrated that, compared with those in the control group, the protein levels of p-AKT (Fig. 4A) and the p-AKT/AKT ratio (Fig. 4B) were significantly decreased in EPCs of the hypoxia group. In comparison with those in the hypoxia + mimic control group, the protein levels of p-AKT (Fig. 4A) and the p-AKT/AKT ratio (Fig. 4B) were significantly increased hypoxia + miR-126 mimic group, which were

all significantly reversed by PIK3R2-plasmid co-transfection (Fig. 4A and B). However, the mRNA expression of AKT did not differ significantly among the six groups (Fig. 4C).

VEGF expression is reduced by hypoxia in EPCs. To further explore the relationship between miR-126 and VEGF in EPCs under hypoxic conditions, the protein and mRNA expression of VEGF were measured. VEGF expression was found to be significantly lower in the hypoxia group compared with that in the control group on both protein and mRNA levels (Fig. 5A-C). In addition, EPCs were transfected with either the control-plasmid or VEGF-plasmid under normal conditions, following which
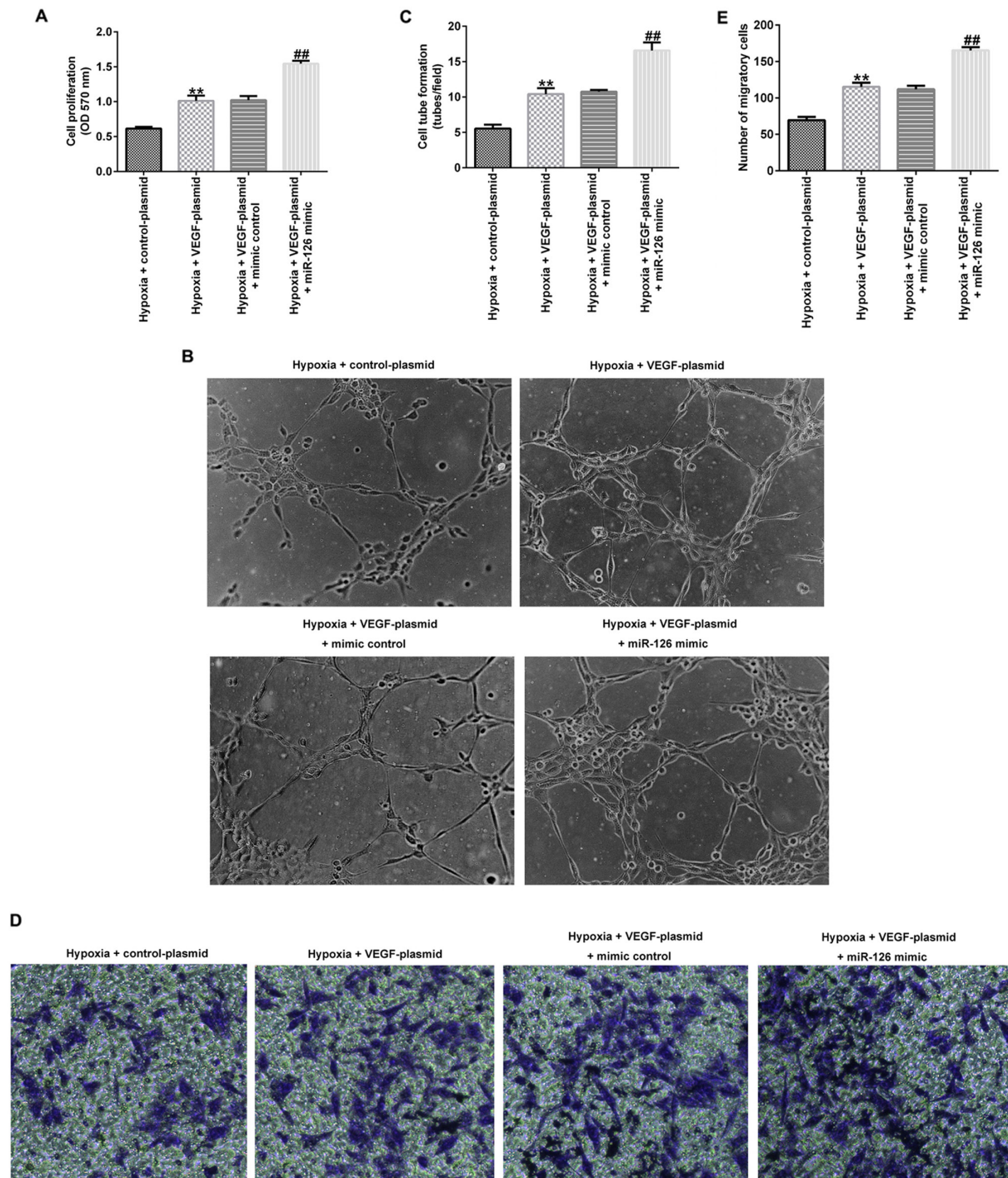
Figure 6. Effects of VEGF and miR-126 mimic transfection on the viability, tube-forming ability and migration of EPCs under hypoxic conditions. EPCs were transfected with control-plasmid, VEGF-plasmid, VEGF-plasmid + mimic control or VEGF-plasmid + miR-126 mimic under hypoxic conditions for 72 h. (A) MTT assay was used to evaluate the cell viability of transfected EPCs. (B) Tube formation assay was performed to measure the tube-forming ability of transfected EPCs. Magnification, x100. (C) Tube formation assay was quantified. (D) Transwell assay was used to measure the migration ability of transfected EPCs Magnification, x200. (E) Transwell assay was quantified. **P<0.01 vs. hypoxia + control-plasmid. ##P<0.01 vs. hypoxia + VEGF-plasmid + mimic control. miR, microRNA; EPCs, endothelial progenitor cells.

it was observed that VEGF-plasmid transfection significantly increased VEGF mRNA levels in EPCs under normal conditions compared with that in cells transected with the control plasmid (Fig. 5D). In addition, EPCs were transfected with either the control-plasmid or VEGF-plasmid under hypoxic conditions, where it was observed that VEGF-plasmid transfection increased the expression of VEGF on both protein and mRNA

levels in EPCs under hypoxic conditions compared with that in cells transected with the control plasmid (Fig. 5E-G).

VEGF overexpression enhances the effects of miR-126 on EPCs under hypoxic conditions. Several experiments were performed after the cells were transfected for 72 h under hypoxic conditions. As shown in Fig. 6A-E, VEGF-plasmid
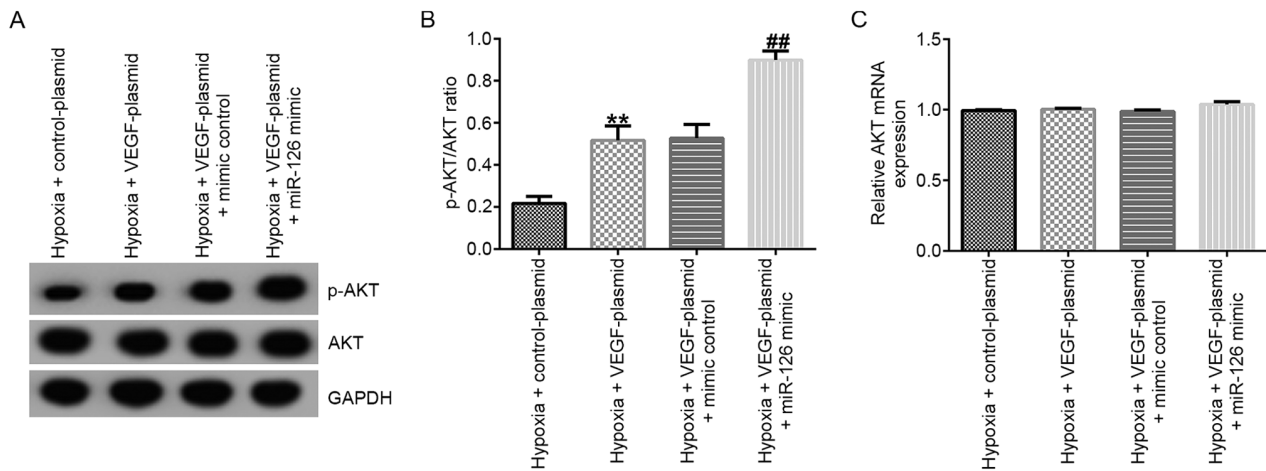
Figure 7. Effects of VEGF and miR-126 mimic transfection on the PI3K/AKT pathway in EPCs under hypoxic conditions. EPCs were transfected with control-plasmid, VEGF-plasmid, VEGF-plasmid + mimic control or VEGF-plasmid + miR-126 mimic under hypoxic conditions for 72 h. (A) Western blot analysis was used to detect the protein levels of p-AKT and AKT in transfected EPCs. (B) p-AKT/AKT ratio was quantified. (C) Reverse transcription-quantitative PCR analysis was used to measure the mRNA expression of AKT in transfected EPCs. **P<0.01 vs. hypoxia + control-plasmid. ##P<0.01 vs. hypoxia + VEGF-plasmid + mimic control group. EPCs, endothelial progenitor cells; miR, microRNA; p-, phosphorylated.

transfection significantly increased the cell viability (Fig. 6A), tube-forming ability (Fig. 6B and C) and migration (Fig. 6D and E) of EPCs under hypoxic conditions compared with those in cells transfected with the control-plasmid. However, co-transfection with the miR-126 mimic significantly potentiated all of these aforementioned effects.

Furthermore, it was observed that transfection with the VEGF-plasmid significantly enhanced the protein levels of p-AKT (Fig. 7A) and the p-AKT/AKT ratio (Fig. 7B) in EPCs under hypoxic conditions compared with those in cells transfected with the control-plasmid. These aforementioned effects were significantly potentiated by co-transfection with the miR-126 mimic. However, VEGF overexpression did not affect the mRNA expression of AKT (Fig. 7C).

Discussion

AMI is one of the main causes of morbidity and mortality worldwide (3,5,32). EPCs are also known as angioblasts and belong to a family of precursor cells in the vascular endothelium (33). Previous studies have shown that EPCs serve an important role in cardiovascular and cerebrovascular diseases, peripheral vascular diseases, tumor angiogenesis and wound healing, where they can potentially provide novel approaches for the treatment of ischemic diseases (34,35). There have also been an increasing number of studies on the biological characteristics and therapeutic effects of EPCs (36,37). The proliferation and migration of endothelial cells serve an important role in maintaining vascular integrity, regeneration and wound repair (38). In particular, miR-126 was previously demonstrated to mediate a key function in maintaining the integrity of endothelial cells, inflammation, angiogenesis and vascular repair (39). EPCs were used to establish an *in vitro* hypoxia model in the present study, where it was verified that miR-126 expression was reduced in EPCs under hypoxic conditions, which is consistent with previous finding (40). However, the phenotypic confirmation of the EPCs by FACS/flow cytometry was not performed in this study, which was a limitation of the present study.

It has been previously reported that PIK3R2, which encodes the p85β regulatory subunit of PI3K, is a target of miR-126 (27,28,41,42). In the present study, it was confirmed that miR-126 can directly target PIK3R2. Therefore, it was hypothesized that miR-126 may regulate the proliferation of EPCs by targeting PIK3R2 expression. To further study the molecular mechanisms through which miR-126 regulates the proliferation of EPCs, the cells were transfected for 72 h and divided into the following groups: Control, hypoxia, hypoxia + mimic control, hypoxia + miR-126 mimic, hypoxia + miR-126 mimic + control-plasmid and hypoxia + miR-126 mimic + PIK3R2-plasmid. MTT, Transwell and tube formation assays were used to detect cell proliferation, migration and tube-forming ability, respectively. It was observed that upregulating miR-126 could promote the viability, migration and tube-forming capabilities of EPCs under hypoxic conditions by downregulating the expression of PIK3R2. Previous studies have shown that miR-126 can upregulate the response of cells to VEGF by directly inhibiting a number of its inhibitors, including Spred-1 and PIK3R2 (43-45). However, whether miR-126 regulates angiogenesis through VEGF during myocardial ischemia remains poorly understood. The relationship between miR-126 and VEGF in the regulation of EPC physiology under hypoxic conditions was investigated in the present study, where the results suggest that VEGF expression was reduced in EPCs under hypoxic conditions and VEGF upregulation enhanced cellular functions (cell proliferation, migration, and tube formation ability) by combining with miR-126.

The PI3K/AKT pathway appears to serve an important role in improving the function of EPCs by regulating the migration and angiogenesis of EPCs (46,47). Previous studies have also reported that miR-126 can regulate PI3K/AKT pathway activation in cancer cells such as non-small cell lung cancer and bladder cancer cells (28,41). However, the possible effects on the PI3K/AKT pathway exerted by changes in miR-126 expression in EPCs under hypoxic conditions remain unclear. Therefore, activities of AKT was measured in this study. It

was found that miR-126 overexpression enhanced AKT activation in EPCs under hypoxic conditions, which was reversed by PIK3R2 overexpression. In addition, it was confirmed that VEGF and miR-126 mediate a synergistic role in promoting the activation of AKT.

However, there were some limitations in the present study. For example, the effects of miR-126 and VEGF overexpression on apoptosis and/or necrosis in EPCs under hypoxic conditions were not investigated. In addition, since the differences in cell viability, tube forming abilities and migration of EPCs were already between the normoxic control and hypoxic condition were already observed, the normoxic control group was not designated in the miR-126 and VEGF-plasmid co-transfection experiments, which would've made the results more credible. In addition, the role of miR-126/VEGF on EPC function in AMI should be studied *in vivo*.

In conclusion, the present study demonstrated that miR-126 overexpression promoted the functions of EPCs under hypoxic conditions by downregulating PIK3R2 expression, where the combination of miR-126 and VEGF overexpression can potentiate these effects. These findings suggest that targeting miR-126 and VEGF may provide novel directions for the clinical treatment of AMI.

Acknowledgements

Not applicable.

Availability of data and materials

The datasets used and/or analyzed during the current study are available from the corresponding author on reasonable request.

Authors' contributions

YZ and JX contributed to study design, data collection and interpretation and statistical analysis. YX, KZ and GK contributed to performing the experiments and statistical analysis. YZ and JX confirm the authenticity of all the raw data. All authors read and approved the final manuscript.

Ethics approval and consent to participate

The present study was approved by the Ethics Committee of Chongqing Emergency Medical Center (Fourth People's Hospital of Chongqing; Chongqing, China).

Patient consent for publication

Not applicable.

Competing interests

The authors declare that they have no competing interests.

References

1. Nichols M, Townsend N, Scarborough P and Rayner M: Cardiovascular disease in Europe 2014: Epidemiological update. Eur Heart J 35: 2950-2959, 2014.
2. Yeh RW, Sidney S, Chandra M, Sorel M, Selby JV and Go AS: Population trends in the incidence and outcomes of acute myocardial infarction. N Engl J Med 362: 2155-2165, 2010.
3. Tibaut M, Mekis D and Petrovic D: Pathophysiology of Myocardial Infarction and Acute Management strategies. Cardiovasc Hematol Agents Med Chem 14: 150-159, 2017.
4. Anderson JL and Morrow DA: Acute myocardial infarction. N Engl J Med 376: 2053-2064, 2017.
5. Gulati R, Behfar A, Narula J, Kanwar A, Lerman A, Cooper L and Singh M: Acute myocardial infarction in young individuals. Mayo Clin Proc 95: 136-156, 2020.
6. Eltzschig HK and Eckle T: Ischemia and reperfusion-from mechanism to translation. Nat Med 17: 1391-1401, 2011.
7. Arora G and Bittner V: Chest pain characteristics and gender in the early diagnosis of acute myocardial infarction. Curr Cardiol Rep 17: 5, 2015.
8. Shah AH, Puri R and Kalra A: Management of cardiogenic shock complicating acute myocardial infarction: A review. Clin Cardiol 42: 484-493, 2019.
9. Abed MA, Ali RM, Abu Ras MM, Hamdallah FO, Khalil AA and Moser DK: Symptoms of acute myocardial infarction: A correlational study of the discrepancy between patients' expectations and experiences. Int J Nurs Stud 52: 1591-1599, 2015.
10. Ndrepepa G, Keta D, Schulz S, Byrne RA, Mehilli J, Pache J, Seyfarth M, Schömig A and Kastrati A: Prognostic value of minimal blood flow restoration in patients with acute myocardial infarction after reperfusion therapy. Clin Res Cardiol 99: 13-19, 2010.
11. Peters EB: Endothelial progenitor cells for the vascularization of engineered tissues. Tissue Eng Part B Rev 24: 1-24, 2018.
12. Naito H, Iba T and Takakura N: Mechanisms of new blood-vessel formation and proliferative heterogeneity of endothelial cells. Int Immunol 32: 295-305, 2020.
13. Li X, Xue X, Sun Y, Chen L, Zhao T, Yang W, Chen Y and Zhang Z: MicroRNA-326-5p enhances therapeutic potential of endothelial progenitor cells for myocardial infarction. Stem Cell Res Ther 10: 323, 2019.
14. Huang H, Xu Z, Qi Y, Zhang W, Zhang C, Jiang M, Deng S and Wang H: Exosomes from SIRT1-Overexpressing ADSCs restore cardiac function by improving angiogenic function of EPCs. Mol Ther Nucleic Acids 21: 737-750, 2020.
15. Zhou W, Zhou W, Zeng Q and Xiong J: MicroRNA-138 inhibits-hypoxia-induced proliferation of endothelial progenitor cells via inhibition of HIF-1α-mediated MAPK and AKT signaling. Exp Ther Med 13: 1017-1024, 2017.
16. Lu TX and Rothenberg ME: MicroRNA. J Allergy Clin Immunol 141: 1202-1207, 2018.
17. Mohr AM and Mott JL: Overview of microRNA biology. Semin Liver Dis 35: 3-11, 2015.
18. Saliminejad K, Khorram Khorshid HR, Soleymani Fard S and Ghaffari SH: An overview of microRNAs: Biology, functions, therapeutics, and analysis methods. J Cell Physiol 234: 5451-5465, 2019.
19. Liu B, Li J and Cairns MJ: Identifying miRNAs, targets and functions. Brief Bioinform 15: 1-19, 2014.
20. Juźwik CA, S Drake S, Zhang Y, Paradis-Isler N, Sylvester A, Amar-Zifkin A, Douglas C, Morquette B, Moore CS and Fournier AE: MicroRNA dysregulation in neurodegenerative diseases: A systematic review. Prog Neurobiol 82: 101664, 2019.
21. Rupaimoole R and Slack FJ: MicroRNA therapeutics: Towards a new era for the management of cancer and other diseases. Nat Rev Drug Discov 16: 203-222, 2017.
22. Sun IO and Lerman LO: Urinary microRNA in kidney disease: Utility and roles. Am J Physiol Renal Physiol 316: F785-F793, 2019.
23. Wojciechowska A, Braniewska A and Kozar-Kamińska K: MicroRNA in cardiovascular biology and disease. Adv Clin Exp Med 26: 865-874, 2017.
24. Johnson JL: Elucidating the contributory role of microRNA to cardiovascular diseases (a review). Vascul Pharmacol 114: 31-48, 2019.
25. Sun J, Zhang Z, Ma T, Yang Z, Zhang J, Liu X, Lu D, Shen Z, Yang J and Meng Q: Endothelial progenitor cell-derived exosomes, loaded with miR-126, promoted deep vein thrombosis resolution and recanalization. Stem Cell Res Ther 9: 223, 2018.

26. Meng S, Cao JT, Zhang B, Zhou Q, Shen CX and Wang CQ: Downregulation of microRNA-126 in endothelial progenitor cells from diabetes patients, impairs their functional properties, via target gene Spred-1. J Mol Cell Cardiol 53: 64-72, 2012.
27. Fu R and Tong JS: MiR-126 reduces trastuzumab resistance by targeting PIK3R2 and regulating AKT/mTOR pathway in breast cancer cells. J Cell Mol Med 24: 7600-7608, 2020.
28. Song L, Li D, Gu Y, Wen ZM, Jie J, Zhao D and Peng LP: MicroRNA-126 targeting PIK3R2 inhibits NSCLC A549 cell proliferation, migration, and invasion by regulation of PTEN/PI3K/AKT pathway. Clin Lung Cancer 17: e65-e75, 2016.
29. Fish JE, Santoro MM, Morton SU, Yu S, Yeh RF, Wythe JD, Ivey KN, Bruneau BG, Stainier DY and Srivastava D: MiR-126 regulates angiogenic signaling and vascular integrity. Dev Cell 15: 272-284, 2018.
30. Ye P, Liu J, He F, Xu W and Yao K: Hypoxia-induced deregulation of miR-126 and its regulative effect on VEGF and MMP-9 expression. Int J Med Sci 11: 17-23, 2013.
31. Livak KJ and Schmittgen TD: Analysis of relative gene expression data using real-time quantitative PCR and the 2(-Delta Delta C(T)) method. Methods 25: 402-408, 2001.
32. Reed GW, Rossi JE and Cannon CP: Acute myocardial infarction. Lancet 389: 197-210, 2017.
33. Ratajska A, Jankowska-Steifer E, Czarnowska E, Olkowski R, Gula G, Niderla-Bielińska J, Flaht-Zabost A and Jasińska A: Vasculogenesis and its cellular therapeutic applications. Cells Tissues Organs 203: 141-152, 2017.
34. Yuan JJ, Yang J, Sun SL, Zhang R and Xu YM: Endothelial progenitor cells' classification and application in neurological diseases. Tissue Eng Regen Med 14: 327-332, 2017.
35. Ma Y, Jiang L, Wang L, Li Y, Liu Y, Lu W, Shi R, Zhang L, Fu Z, Qu M, *et al*: Endothelial progenitor cell transplantation alleviated ischemic brain injury by inhibiting C3/C3aR pathway in mice. J Cereb Blood Flow Metab 40: 2374-2386, 2020.
36. Steinle H, Golombek S, Behring A, Schlensak C, Wendel HP and Avci-Adali M: Improving the angiogenic potential of EPCs via engineering with synthetic modified mRNAs. Mol Ther Nucleic Acids 13: 387-398, 2018.
37. Zeng YC, Peng LS, Zou L, Huang SF, Xie Y, Mu GP, Zeng XH, Zhou XL and Zeng YC: Protective effect and mechanism of lycopene on endothelial progenitor cells (EPCs) from type 2 diabetes mellitus rats. Biomed Pharmacother 92: 86-94, 2017.
38. Klein-Soyer C, Beretz A, Cazenave JP, Driot F and Maffrand JP: Behavior of confluent endothelial cells after irradiation. Modulation of wound repair by heparin and acidic fibroblast growth factor. Biol Cell 68: 231-238, 1990.
39. Chen G, Li P, Liu Z, Zeng R, Ma X, Chen Y, Xu H, Li Z and Lin H: Enrichment of miR-126 enhances the effects of endothelial progenitor cell-derived microvesicles on modulating MC3T3-E1 cell function via Erk1/2-Bcl-2 signalling pathway. Prion 13: 106-115, 2019.
40. Pan Q, Zheng J, Du D, Liao X, Ma C, Yang Y, Chen Y, Zhong W and Ma X: MicroRNA-126 priming enhances functions of endothelial progenitor cells under physiological and hypoxic conditions and their therapeutic efficacy in cerebral ischemic damage. Stem Cells Int 2018: 2912347, 2018.
41. Xiao J, Lin HY, Zhu YY, Zhu YP and Chen LW: MiR-126 regulates proliferation and invasion in the bladder cancer BLS cell line by targeting the PIK3R2-mediated PI3K/Akt signaling pathway. Onco Targets Ther 9: 5181-5193, 2016.
42. Yang WZ, Yang J, Xue LP, Xiao LB and Li Y: MiR-126 overexpression inhibits high glucose-induced migration and tube formation of rhesus macaque choroid-retinal endothelial cells by obstructing VEGFA and PIK3R2. J Diabetes Complications 31: 653-663, 2017.
43. Li SN, Li P, Liu WH, Shang JJ, Qiu SL, Zhou MX and Liu HX: Danhong injection enhances angiogenesis after myocardial infarction by activating MiR-126/ERK/VEGF pathway. Biomed Pharmacother 120: 109538, 2019.
44. Zhang L, Ouyang P, He G, Wang X, Song D, Yang Y and He X: Exosomes from microRNA-126 overexpressing mesenchymal stem cells promote angiogenesis by targeting the PIK3R2-mediated PI3K/Akt signalling pathway. J Cell Mol Med 25: 2148-2162, 2021.
45. Nammian P, Razban V, Tabei SMB and Asadi-Yousefabad SL: MicroRNA-126: Dual role in angiogenesis dependent diseases. Curr Pharm Des 26: 4883-4893, 2020.
46. Chen X, Chen Q, Wang L and Li G: Ghrelin induces cell migration through GHSR1a-mediated PI3K/Akt/eNOS/NO signaling pathway in endothelial progenitor cells. Metabolism 62: 743-752, 2013.
47. Li WD, Zhou DM, Sun LL, Xiao L, Liu Z, Zhou M, Wang WB and Li XQ: LncRNA WTAPP1 promotes migration and angiogenesis of endothelial progenitor cells via MMP1 through MicroRNA 3120 and Akt/PI3K/autophagy pathways. Stem Cells 36: 1863-1874, 2018.